Quill
RADAR

KP-II
PROGRAM REPORT

AKP-II-596 /Vol I

1 APRIL 1965

SSF-II-1018-1

~~SECRET~~
SPECIAL HANDLING

HANDLE VIA BYEMAN CONTROL SYSTEM ONLY

COPY NO. 17

KP-II
PROGRAM REPORT

KP-II ORBITAL DOPPLER RADAR
THOR/AGENA SATELLITE PROGRAM

VOLUME I - DESIGN AND DEVELOPMENT

AKP-II-596

1 APRIL 1965
S

This document contains 180 pages classified as SECRET: SPECIAL HANDLING

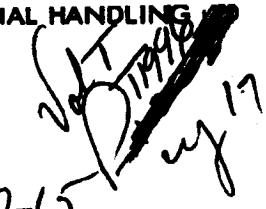

GOODYEAR AEROSPACE CORPORATION
ARIZONA DIVISION LITCHFIELD PARK, ARIZONA

This page intentionally left blank.

FOREWORD

This report is submitted in response to the requirements of Air Force Contract [redacted]. Documented herein is the design, development, and testing phases of the KP-II Orbital Doppler Radar produced by Goodyear Aerospace Corporation, Litchfield Park, Arizona. The period covered is from 15 January 1963 to 1 April 1965.

Prepared by:

[redacted]
Project Engineer

Approved:

David D. Bradburn
Lt. Col., USAF
SAFSP

This page intentionally left blank.

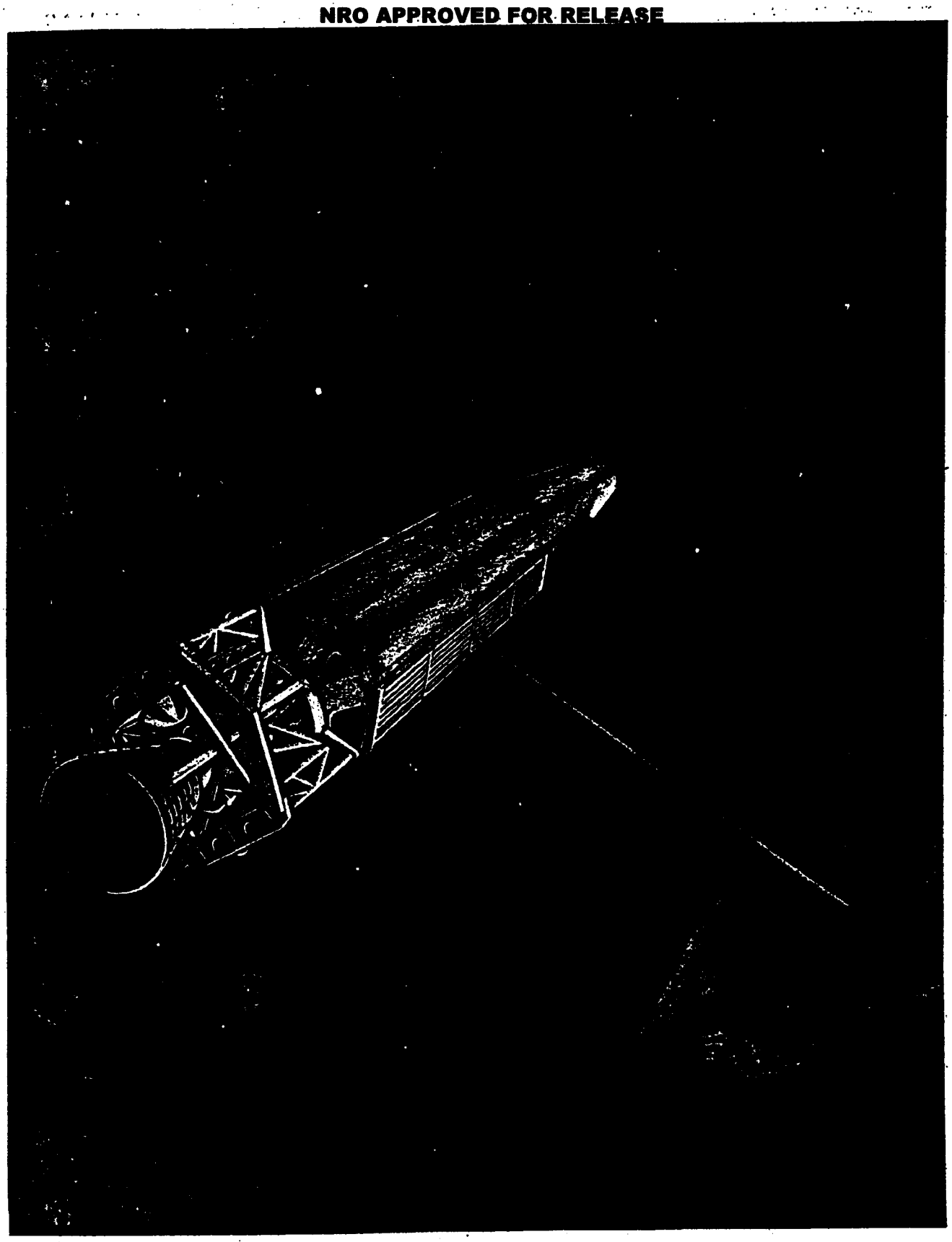

This page intentionally left blank.

TABLE OF CONTENTS

TABLE OF CONTENTS

LIST OF ILLUSTRATIONS

LIST OF TABLES

SECTION I - INTRODUCTION

1. GENERAL

In January, 1963, Goodyear Aerospace Corporation, Arizona Division, was contracted by the Secretary of the Air Force Special Projects Office (SAFSP) to participate in an Agena Vehicle Satellite Program. The primary objective of the program was to demonstrate the feasibility of obtaining doppler high-resolution radar imagery of the earth's terrain from an orbiting satellite. To accomplish this objective, it was proposed to base the radar system, wherever practical, upon the existing designs of the Goodyear-produced AN/UPQ-102 side-looking doppler radar.

Initial studies and proposal efforts on this program had previously begun in the latter part of 1962 when a number of meetings were held between Goodyear Aerospace, Lockheed Missile and Space Company (LMSC), and the [redacted] to discuss system parameters, design concepts, and vehicle configuration. Actual work on the radar portion of the program began at Goodyear Aerospace on January 15, 1963. Twenty-three months later on December 21, 1964, successful completion of the first orbital radar test was achieved.

This program report is divided into two volumes. This volume – Volume I – documents the initial system analysis, design, and development of the Goodyear KP-II side-looking doppler radar system. Volume II describes the ground tests to which the system was subjected, and presents the results of the orbital flight test.

2. DESIGN PHILOSOPHY

To accomplish the program objective, extensive changes were required to the existing designs of the AN/UPQ-102 doppler radar. The KP-II radar was required to operate at 20 times the ground speed and 16 times the altitude of the AN/UPQ-102 radar. The KP-II radar was required to scan one side only; the AN/UPQ-102 radar scanned on both sides and used two receiving and recording channels. In the AN/UPQ-102 radar, the film speed and prf were slaved to

ground speed; in the KP-II radar they would be constant. Additionally, the AN/UPQ-102 radar incorporated many modes of operation, such as moving target indication and variable mapping intervals, which were not included in the requirements for the KP-II radar. Finally, the more difficult vibration and pressure requirements of the satellite environment would necessitate an extensive repackaging of the radar units.

It was decided that specialized parts, such as klystrons, traveling wave tubes, cathode ray tubes, and frequency multipliers, would be procured from previously established vendors wherever possible. To ensure that these specialized parts would meet all requirements, new specification control drawings were made and the components procured to these specifications.

It was also decided that the payload would be instrumented in such a manner that flight performance and failure mode data could be obtained from narrow band telemetry information.

3. CONFIGURATION

The KP-II radar payload equipment which was designed and built by Goodyear Aerospace consists of the following units: Transmitter, RF-IF, Reference Computer, Control, and Recorder. The equipment, with the exception of the recorder, is installed in the forward barrel section of a standard Agena D vehicle. The recorder is installed in the conical nose section directly behind the film recovery capsule. The radar antenna, built by LMSC, is attached to the side of the Agena vehicle and is a two-dimensional slotted wave guide array. The antenna is 15 feet long, 1.8 feet in height, and is uniformly illuminated in both directions.

4. SYSTEM PARAMETERS

The radar payload is designed to operate at an altitude of 130 ±13 nautical miles. The orbital inclination angle is 70 degrees. A fixed radar depression angle of 55 degrees is used. The radar maps a slant range interval of 5.95 nautical miles which is independent of altitude variation. This slant range interval corresponds to a ground range interval of approximately 10 miles.

The design value for peak transmitter power is 30 kilowatts and the average transmitter power is 262 watts. The length of the transmitter pulse is 1.0 microsecond. By the use of pulse compression techniques this is reduced to an effective pulse width of 0.06 microsecond. The minimum acceptable resolution for the system is 50 feet slant range resolution and 50 feet azimuth resolution. Actual system performance was found to be better than these minimum acceptable values.

The pulse repetition frequency (prf) has a 16-step variable range from 8215 to 8735. Changes in prf are accomplished via the payload command system. A grey code is used to allow a one-step change in prf to be accomplished by a single command. During flight, change of prf from its preprogrammed position was made on the basis of the radar data received at the tracking station.

The total power consumed by the radar system in the operate mode is 2500 watts. The total weight of the five payload components is 348 pounds.

5. OPERATIONAL SUMMARY

The payload was launched by a thrust-augmented Thor booster and had a useful orbital life of approximately four days.

Radar radiation was confined (1) to the limits of the continental United States, and (2) to the limits of control of the Vandenburg and New Boston tracking stations. Doppler radar data were recorded simultaneously by the recorder unit contained in the vehicle and also by a ground-based recorder located at the tracking station. The data were transmitted to the controlling tracking station via a wide-band data link. There were a total of 14 mapping passes within the four-day period. The time interval for each pass varied from 1.4 to 3.7 minutes. The total mapping time was 32.91 minutes. The unprocessed vehicle data film was returned to earth in the recovery capsule. The resulting high-resolution imagery from the data films confirms the feasibility of doppler high-resolution radar techniques for space application.

6. CHRONOLOGY OF PROGRAM HISTORY

To give chronological perspective to the design and development phases of the program, a summary of events on a monthly basis is included as Appendix I to this volume.

SECTION II - BASIC DOPPLER THEORY

1. GENERAL CONCEPT

The beam-sharpening process used in a doppler, high-resolution, side-looking radar may be described by means of a physical antenna analog. As the vehicle travels its orbital path a series of pulses is transmitted. Successive pulse transmissions are identified with the elements of an array of dipoles. The spacing between elements is the distance traveled by the vehicle between pulses. Each transmission is made with a controlled phase. The amplitude and phase of the reflected energy from the terrain at all ranges and angles within the physical beam width of the antenna is recorded on the data film.

The length of the antenna synthetically generated is basically limited to the distance instantaneously illuminated on the ground by the physical antenna. By the technique of optical processing, the amplitude and phase of the returns from the successive pulses are vectorially added to create the narrow synthetic beam. The results of these data are then recorded on a final film. Thus, the resolution equivalent to that of an antenna hundreds of feet in length is achieved with a small physical antenna.

2. BASIC EQUATIONS

The basic equations of a high-resolution radar are most easily developed if the analysis is restricted to the slant-range plane of a single-point target. Figure 1 shows the geometry involved. R is the distance to the target from the antenna at time t. At time t = 0, R_1 is the distance to the target. The angle θ_o is measured in the slant-range plane to the center of the antenna beam at slant range R_1. Several combinations of pitch and yaw will yield the same angle θ_o.

From the geometry of Figure 1 the instantaneous range R to the target is

$$R = \left[R_1^2 + (vt)^2 - 2R_1 vt \sin \theta_o\right]^{1/2} . \qquad (1)$$

As the beam width of the physical antenna is small, the range during the period when the target is illuminated may be closely approximated by taking the first few terms of the binomial expansion of Equation (1):

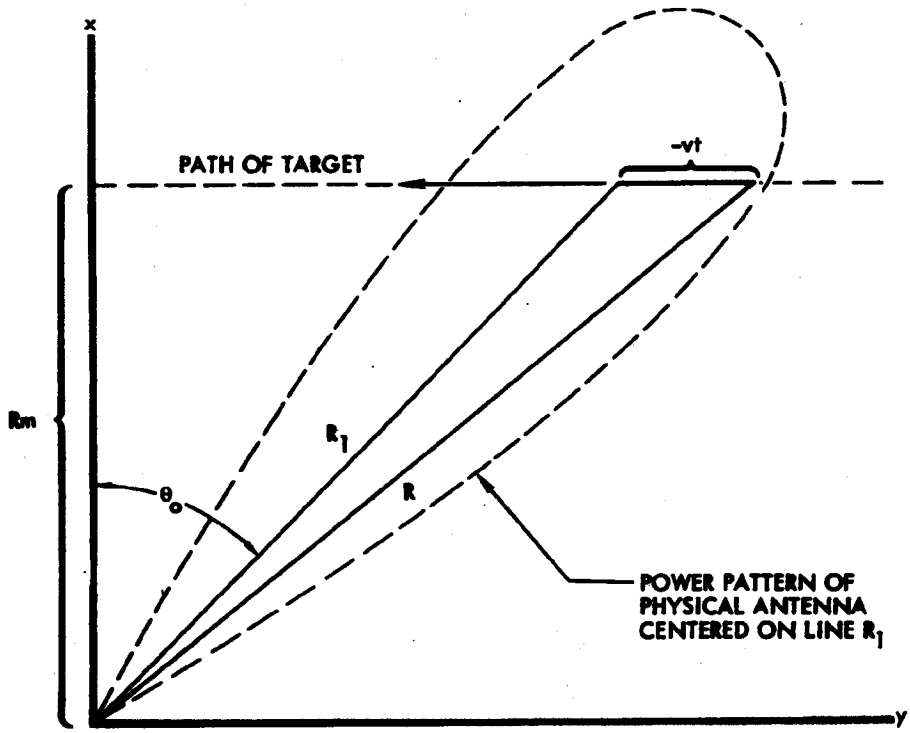

2226-57

Figure 1 - Geometry of a Point Target in the Slant Range Plane

$$R \approx R_1\left(1 - \frac{vt \sin \theta_o}{R_1} + 1/2 \frac{(vt)^2}{R_1^2} \cos^2 \theta_o\right) . \quad (2)$$

The range dependence on time is reflected in a phase dependence on time of the return signal. The dependence of phase ϕ of the return signal on time is

$$\phi = 2\pi f_o t - \frac{4\pi R}{\lambda} + \phi_o \quad (3)$$

where

f_o = the transmitted frequency

λ = the wave length of the carrier

ϕ_o = the phase change caused by reflection.

Equations (2) and (3) may be developed into

$$\phi = 2\pi f_o t + \frac{4\pi}{\lambda} vt \sin \phi_o - \frac{2\pi(vt)^2}{R_1 \lambda} \cos^2 \phi_o + \phi_1 \quad (4)$$

where

$$\phi_1 = \phi_o - \frac{4\pi R_1}{\lambda} .$$

The return signal is synchronously demodulated with respect to some reference frequency to remove the carrier. It is desirable for the reference frequency to be the frequency of the return signal when the target is at the center of the beam. The phase of the return signal when the target is at the center of the beam and at range R_1 is given by

$$\gamma = 2\pi f_o t - \frac{4\pi R_1}{\lambda} + \phi_o . \quad (5)$$

The frequency will be

$$f_r = \frac{1}{2\pi} \frac{d\gamma}{dt} = \frac{1}{2\pi}\left(2\pi f_o - \frac{4\pi}{\lambda} \frac{dR_1}{dt}\right) . \quad (6)$$

From Figure 1, however,

$$\frac{dR_1}{dt} \equiv \frac{dR}{dt}\Big|_{t=0} \quad . \tag{7}$$

Therefore, from Equation (2)

$$\frac{dR_1}{dt} = -v \sin \theta_o \quad . \tag{8}$$

Then, substituting into Equation (6),

$$f_r = f_o + \frac{2v}{\lambda} \sin \theta_o \quad . \tag{9}$$

Therefore, f_r is the frequency that will be used for synchronous demodulation. The synchronous demodulated signal will have the form

$$S(t) = A(t)\mathrm{Re}\left[e^{-j2\pi f_r t}(e^{j\phi})\right] \tag{10}$$

$$= A(t)\cos\left(\frac{2\pi(vt)^2 \cos^2 \phi_o}{R_1 \lambda} - \phi_1\right) \tag{11}$$

where A(t) denotes the amplitude of the return which is a function of the reflectivity of the target and its position in the antenna beam. When

$$\phi_1 = n(2\pi)$$

$$\theta_o = 0$$

and

$$A(t) = K$$

Equation (12) reduces to the familiar expression

$$S(t) = K \cos\left(\frac{2\pi(vt)^2}{\lambda R_m}\right) . \qquad (12)$$

The signal recorded on film at range R_m will be of the form

$$S(x, R_m) = T_b + K' \cos\left(\frac{2\pi x^2}{\lambda R_m}\right) \qquad (13)$$

where

T_b = the transmissivity of the film

K' = some constant times K.

From Equation (9) it is seen that all scatterers at an angle θ_o and with velocity v will have the same frequency. It follows that the locus of all possible scatterers whose returns have the same frequency is one nappe of a right circular cone with semi-apex co-angle θ_o whose axis contains the velocity vector.

The locus of points on the earth can be visualized if the intersection of the above doppler cone with a plane tangent to the earth at midmapping range is considered Since the range interval mapped is small, the mathematical model so described is a good approximation near the point of tangency.

3. AMBIGUITIES

Two types of ambiguities – range and azimuth – are inherent in a coherent high-resolution radar and provisions must be made to avoid them. The range-ambiguity problem is common to all pulsed radar and is usually avoided by lowering the prf so that the so-called "second-time-around" targets are not seen by the radar. However, the consideration of azimuth ambiguities yields another set of constraints on the choice of prf.

For a processor operating about zero doppler the information spaced at $\pm\gamma_n$ from zero doppler is ambiguous. This angular spacing is given by

$$\gamma_n = \frac{n\lambda F}{2v} \tag{14}$$

where

n = a positive integer, 1, 2, 3, . . .

λ = carrier wave length

F = prf

v = radar velocity.

The focused processor used with this system operates about an offset of prf/4 and is unable to distinguish between positive- and negative-going frequencies so that the ambiguity spacing is given by

$$\gamma_n = \frac{n\lambda F}{4v} \tag{15}$$

For most high performance radars it is desirable to choose a prf such that the first azimuth ambiguity is placed in the vicinity of the first null of the physical antenna azimuth pattern. This choice of prf places an upper bound on the size of the mapped interval. This constraint in turn dictates the antenna height, since from the range-ambiguity standpoint the vertical antenna pattern is employed to avoid range ambiguities. It is readily deduced that ambiguity constraints are a determining factor in choosing antenna dimensions for a satellite radar. These considerations will be discussed further in Section III.

4. DATA PROCESSORS

The most successful type of high-resolution processor thus far is the optical correlator.* Considerable insight into the optical processor is possible if

*These devices are commonly known as correlators because the original conception, developed at the University of Michigan, was an optical cross-correlator.

the properties of a sine wave diffraction grating are considered. Figure 2 shows the three principal emergent rays from a sine-wave diffraction grating resulting from an incident plane wave of coherent light. The angle θ is defined thus:

$$\sin \theta = \lambda' f \tag{16}$$

where

λ' = the wave length of the coherent light

f = the spatial frequency of the sine-wave diffraction grating.

Now consider a diffraction grating of the form $\cos (2\pi x^2/\lambda' R_m)$. This is of the same form as the demodulated return signal from a point target (Equation (13). Assuming a one-to-one scale factor in recording the demodulated return, the spatial frequency is $2x/\lambda' R_m$. From Figure 3 the distance r to the crossing of the zero axis is given by

$$r = \frac{x}{\tan \theta} \quad . \tag{17}$$

For small angles

$$\tan \theta = \sin \theta = \theta \quad . \tag{18}$$

Then,

$$r = \frac{x}{\lambda' f} = \frac{x \lambda' R_m}{\lambda' 2x} = \frac{R_m}{2} \tag{19}$$

which is to say that the diffracted light focuses on the zero (doppler) axis at a distance $R_m/2$ from the grating (data film).

From Figure 2 it is recalled that there are three principal emergent waves. For the cosine x^2 grating the three waves are defined thus (see Figure 4):

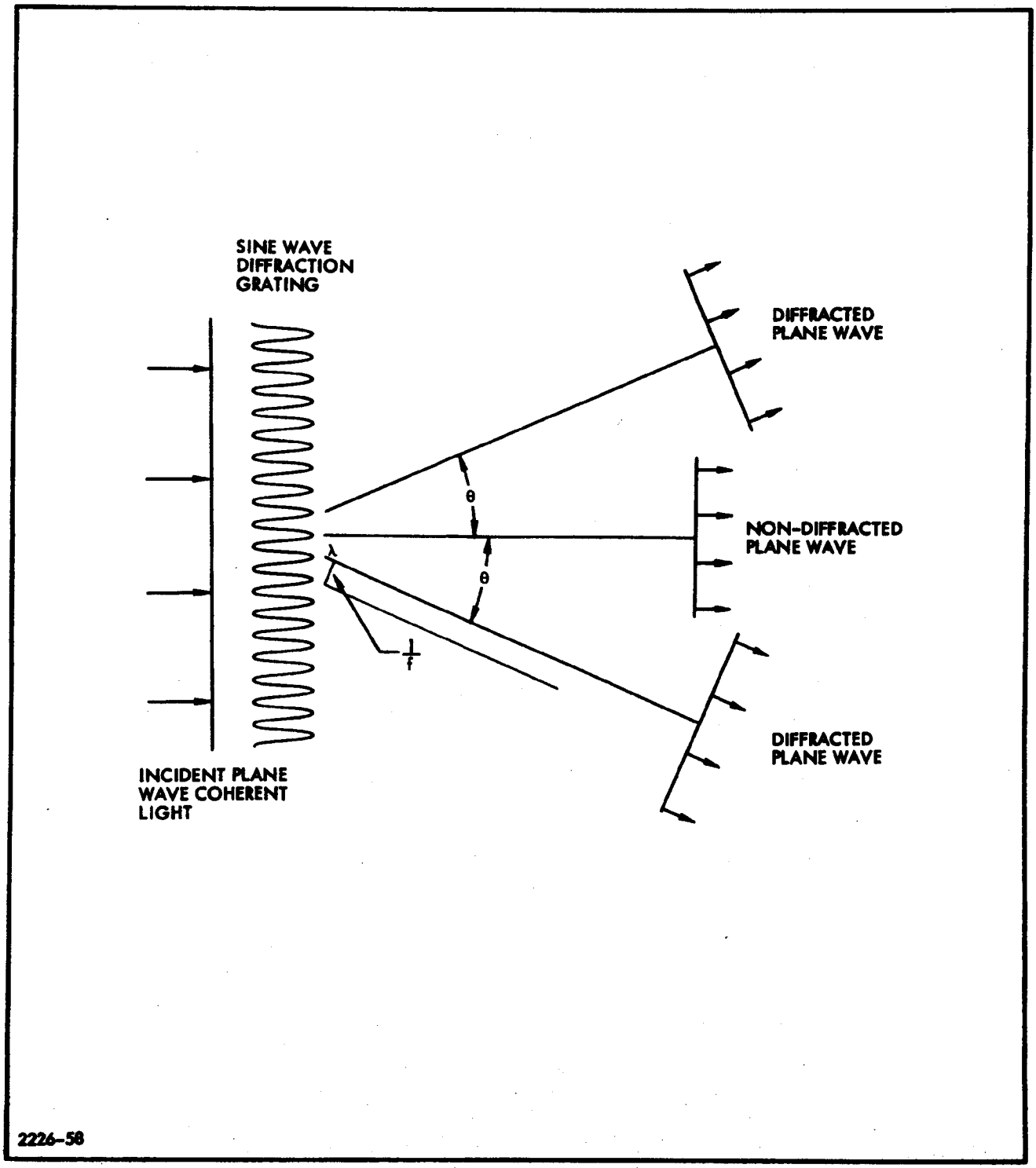

Figure 2 - Geometry Illustrating Fruenhofer Diffraction

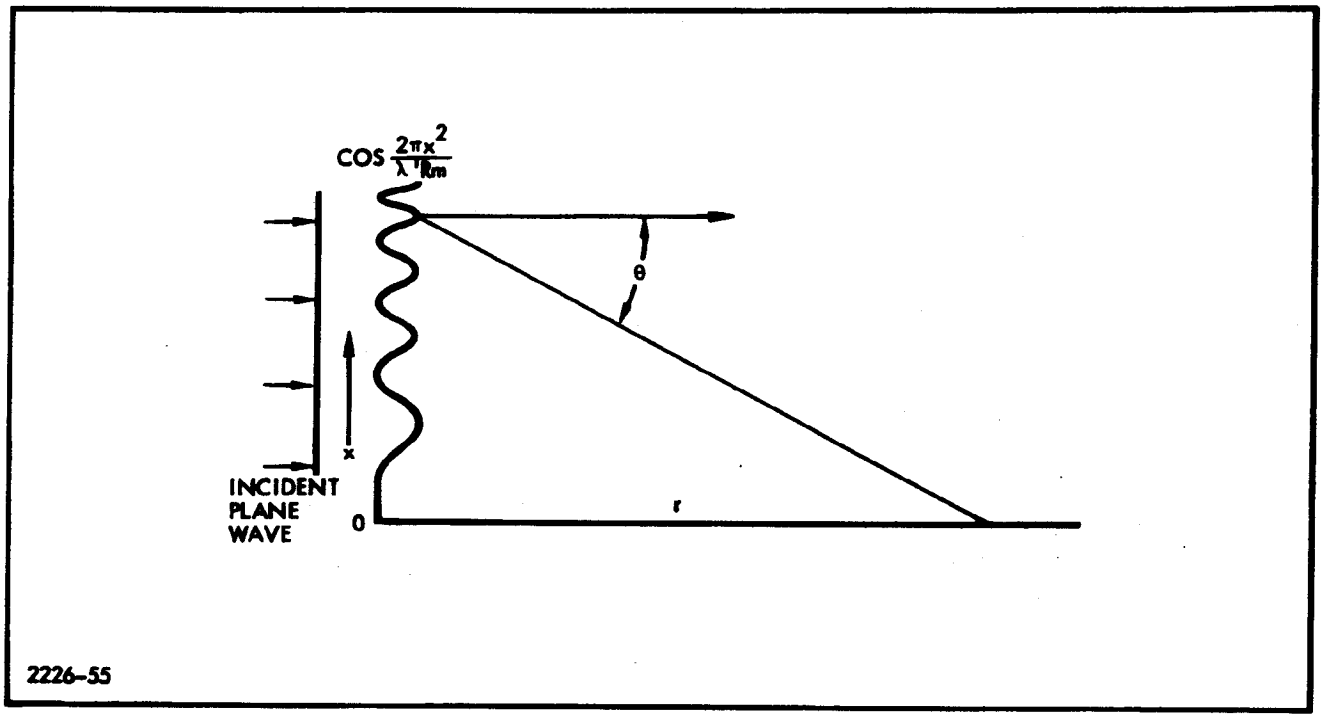

Figure 3 - Diffraction from $\frac{\cos 2\pi x^2}{\lambda' R_m}$ Grating

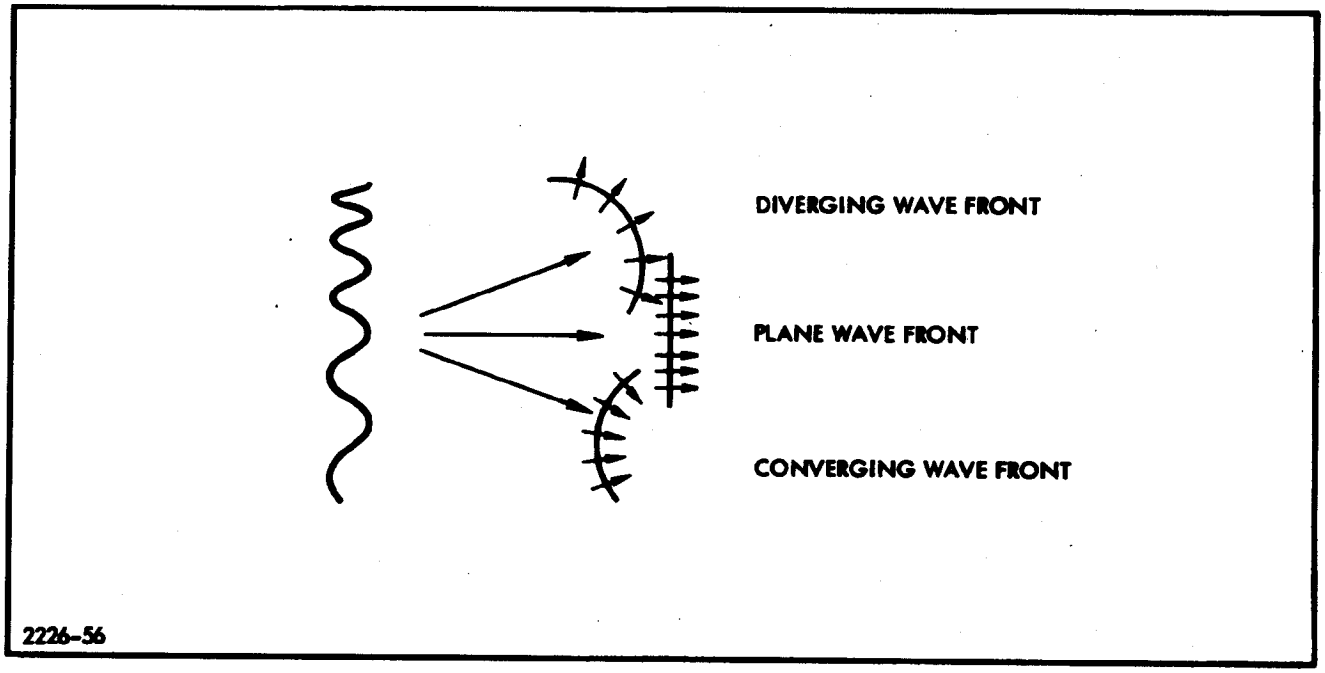

Figure 4 - Three Wave Fronts of a Parabolic Phase History

1. Converging wave front focused at a distance r on the axis
2. Diverging wave front with a virtual image at a distance -r on the axis
3. Plane wave front focused at infinity.

The converging wave front focuses at that angle and at that distance away from the recorded phase history which corresponds to the same angle and the scaled-down distance (proportional to the ratio of light-to-radar wave lengths and aircraft motion-to-film-scale factors) of the radar space where the data were recorded. Unfortunately, in a practical case the ratio is not nearly high enough and a converging lens must be used to bring the desired spot into focus at a convenient distance. Of course the other two wave fronts also come to a focus then but since they lie at different angles they can be blocked off from the final film with an appropriate optical stop. However, from Equation (19), the focal distance is a function of range; therefore, the lens must have a converging power which varies with range, giving rise to a conical shape. A cylindrical lens is also required to maintain target separation in range.

Thus, the basic elements of an optical processor are a coherent light source, optics to focus range and azimuth data onto a single plane, and film drives for transporting both the data and image films.

The optical processor for this system is being provided by the [redacted]

SECTION III - SYSTEM ANALYSIS

1. ANTENNA LENGTH RELATIONSHIPS

Equation (9) demonstrated that the basic equation for the doppler frequency of a scatterer is

$$f_d = \frac{2V_r}{\lambda} \sin \theta \tag{20}$$

where

V_r = relative velocity

λ = radar wave length

θ = angle to scatterer measured from the perpendicular to the relative velocity vector.

Using Equation (20) with Equation (15) and the small angle approximation, the first ambiguous frequency is seen to be F/2. To avoid illumination of this frequency it should be placed at or beyond the first null of the physical antenna pattern. Using this criterion,

$$\frac{F}{2} = \frac{2V_r}{\lambda} \sin \frac{K_a \lambda}{D} \tag{21}$$

or

$$F \approx \frac{4V_r K_a}{D} \tag{22}$$

where

K_a = constant greater than unity

D = length of physical antenna.

The value of K_a varies depending on the type of antenna illumination used in the horizontal plane and the degree of suppression of azimuth ambiguity that is desired.

The basic equation for conditions of range ambiguity is

$$F = \frac{C}{2\Delta R_s \text{ max}} \tag{23}$$

where ΔR_s max = maximum unambiguous slant range interval. Equation (23) assumes a vertical antenna pattern which has a square-shaped beam illuminating only the desired slant range interval. To account for the actual vertical beam shape, Equation (23) may be rewritten as

$$F = \frac{C}{2K_r \Delta R_s} \tag{24}$$

where

K_r = constant greater than unity

ΔR_s = slant range interval mapped.

The value of K_r varies depending on the type of antenna illumination used in the vertical plane and the degree of suppression of range ambiguity which is desired. By using Equations (22) and (24) and solving for ΔR_s, the following relationship is obtained:

$$\Delta R_s = \frac{CD}{8K_a K_r V_r} \quad . \tag{25}$$

This equation shows that the slant range interval which can be mapped is directly proportional to the length of the physical antenna. It is also seen that increasing K_a or K_r to reduce ambiguity levels will reduce the interval mapped.